scientific reports

OPEN

Scientific investigation of a fractional model based on hybrid nanofluids with heat generation and porous medium: applications in the drilling process

Dolat Khan[1], Poom Kumam[2,3]✉, Ilyas Khan[4], Arshad Khan[5], Wiboonsak Watthayu[1] & Muhammad Arif[1]

This article investigates graphite-aluminum oxide hybrid nanoparticles in water-base fluid with the addition of heat generation in the presence of a porous medium. The problem is formulated in terms of momentum and energy equations with sufficient initial and boundary conditions. The solution is investigated by using the Laplace transform method. It is observed that the velocity of the drilling fluid is controlled by adding hybrid nanoparticles as compared to simple nanofluids. In a similar way, the temperature of the fluid is reduced. Also, the heat transfer rate is boosted up to 37.40741% by using hybrid nanofluid compared to regular nanofluid. Moreover, the heat transfer rate was increased up to 11.149% by using different shapes of nanoparticles in the base fluid water. It is also observed that by using hybrid nanofluid skin fraction is boosted up at y = 0 and boosted down at y = 1.

List of symbols

C_p	Heat capacity at a constant pressure, $\text{kg}^{-1}\ \text{K}^{-1}$
k_1	Dimensionless porosity parameter
Gr	Thermal Grashof number
g	Acceleration due to gravity, m s^{-2}
K	Base fluid thermal conductivity, $\text{W m}^{-1}\ \text{K}^{-1}$
B_0	Applied magnetic field, T
σ	Electrical conductivity, $\left(\frac{\text{S}}{\text{m}}\right)$ S is Siemens
Pr	Prandtl number
t	Time, s
u	Velocity of the fluid, m s^{-1}
Q	Heat generation
M	Magnetic parameter
Al_2O_3	Aluminium oxide
$\vec{B}$	Magnetic flux intensity, A m^{-1}
μ_0	Magnetic permeability, N A^{-1}
σ_0	Electrical conductivity, S m^{-1}
i	Unit vector
β_Θ	Volumetric coefficient of thermal expansion, K^{-1}
θ	Dimensionless temperature

[1]Department of Mathematics, Faculty of Science, King Mongkut's University of Technology Thonburi (KMUTT), 126 Pracha Uthit Rd., Bang Mod, Thung Khru, Bangkok 10140, Thailand. [2]Center of Excellence in Theoretical and Computational Science (TaCS-CoE), Faculty of Science, King Mongkut's University of Technology Thonburi (KMUTT), 126 Pracha Uthit Rd., Bang Mod, Thung Khru, Bangkok 10140, Thailand. [3]Department of Medical Research, China Medical University Hospital, China Medical University, Taichung 40402, Taiwan. [4]Department of Mathematics, College of Science Al-Zulfi, Majmaah University, Al-Majmaah 11952, Saudi Arabia. [5]Institute of Computer Sciences and Information Technology, The University of Agriculture, Peshawar, Pakistan. ✉email: poom.kum@kmutt.ac.th

Θ	Temperature of the fluid, K
Θ_∞	Ambient temperature, K
Θ_w	Wall temperature K is used as a unit as well as thermal conductivity, K
$[\cdot]_f$	Base fluid
$[\cdot]_{nf}$	Nanofluid
$[\cdot]_{s1,s2}$	Solid particles
ρ	Density, kg m^{-3}
ϕ	Nanoparticle volume fraction
μ	Dynamic viscosity, kg m^{-1} s^{-1}
Gr	Graphite
d	Distance between two plates, m
$\vec{E}$	Electric field intensity, V m^{-1}
$\vec{J}$	Current density, A m^{-2}
$\vec{V}$	Velocity vector

Heat transfer plays an important role in several manufacturing industries, hearing transition procedures. In the recent era of research, some researchers report the analysis of heat transfer in different fluids which is solved by exact analysis and numerical techniques[1–5]. In various heat transfer systems, fluids such as water, ethylene glycol, alcohol, and oils are known as heat carriers. But because of the low thermal conductivity, they are not a strong heat carrier for these fluids. The scientist's key task was to increase the thermal conductivity of the fluids[6]. One of the approaches normally used in practice to deal with this problem is to maximize the heat exchanger's contact area. However, this approach takes to an unnecessary rise and scientific futility of heat control in the system of heat transport. To control this situation, Choi[7] was the first, who introduced the idea of nanofluids for the improvement of thermal conductivity. From this motivation, many researchers have involved nanofluids in their research to improve the thermal conductivity of fluids in daily life problems[8–12]. Among them, Sheremet et al.[13] reported Aluminium oxide water nanofluids for the application of solar collectors, where the problem is solved by a numerical scheme named the finite difference method. Furthermore, Ali et al.[14] find the exact analysis of nanofluids through the Laplace transform method. They used different types of nanoparticles i.e., Aluminium oxide, titanium oxide, copper oxide, etc. in rotating frames for the application of solar collectors, to improve the efficiency of solar collectors. Krishna and Chamkha[15] used nanofluids for the application in biomedical engineering along with the Hall effects on magnetohydrodynamic (MHD) unsteady flow, which helps in the cancer treatment process. Molana[16,17] added a comprehensive review on nanofluids as an application in heat exchangers and for the performance of thermal enhancement. The authors reported the information on the size and materials of nanoparticles, length, base fluid, flow regime, Reynolds number, and concentration used during research. Sajid and Ali[18] reported a critical review of nanofluids, on the application of advanced and more recently used heat transfer devices. The results of different parameters on the improvement of thermal conductivity using nanofluids have been studied for the devices. Heat transfer equipment mentioned in this study includes a rotating tube, radiators, heat exchangers, tube heat exchangers, heat sinks, and shells. Various associations are often compiled, correlated, and analyzed, which are used for investigational verification or established in reviewed studies. Because normal fluids have low thermal conductivity as compared to nanofluids. As for the formation of ions, nanomaterials are used to improve the expertise in the heat transfer of normal fluids, which subsequently upsurges thermal conductivity. Since then, multiple progressions have been tracked by nanofluids, with various classes.

By preparing hybrid (composite) nanoparticles, the thermal conductivity of the nanoparticles can be altered or modified. Hybrid nanofluids are classified as base fluids that consist of two or more distinct nanometer-sized materials. A brief review of the preparation, heat transfer, friction factor, and thermal properties are reported by Sundar et al.[19]. Sidik et al.[20] reported the method of planning, thermophysical properties, the efficiency of hybrid nanofluid heat transfer, and method of stability investigation in various applications of heat transfer. In addition, this report discusses hybrid nanofluid problems and several recommendations to enhance future studies in this area. Ghadikolaei et al.[21] examined the mathematical analysis of hybrid nanofluid over a stretching sheet along with MHD. The combination of titanium dioxide and copper nanoparticles is taken along with water as base fluid. The solution is obtained via Runge–Kutta (R–K) Fehlberg method. Furthermore, in the recent era, many researchers have used different hybrid nanofluids with different combinations of nanoparticles for various applications. Recently, some of them are, Yildiz et al.[22], Hayat and Nadeem[23], Muhammad[24], Khan et al.[25], etc. Moreover, Khan et al.[26] used clay nanoparticles along with heat transfer to the water cleaning process. The problem was solved by using the Laplace transform method. To investigate the combined effects of heat and mass transfer on the flow of water functionalized oxide and non-oxide nanofluids across porous media, as well as thermal radiation and chemical reaction effects in MHD, is reported by Hussanan et al.[27]. Authors used here three types of basic fluids: water, kerosene, and motor oil, all of which include various forms of oxide and non-oxide nanoparticles. Combining copper (Cu)–Aluminium oxide (Al2O3)/water hybrid nanofluid and magnetic field to investigate the thermal efficacy of half-sinusoidal nonuniform heating at different spatial frequencies for a porous natural convection system is reported by Biswas et al.[28]. Some other researchers also studied water-base hybrid nanofluid for different purposes in different fields[29–32].

As mentioned above, it is very clear that hybrid nanofluid has numerous applications in different fields. Besides this motivation, the novelty of this paper is to examine the scientific investigation of fractional mathematical analysis of hybrid nanofluid as an application in the water filtration process. For this purpose, the combination of graphite and aluminium oxide nanoparticles with water-based fluid is considered in the existence of porous medium and heat generation. The exact solution is investigated by the Laplace transform method. For
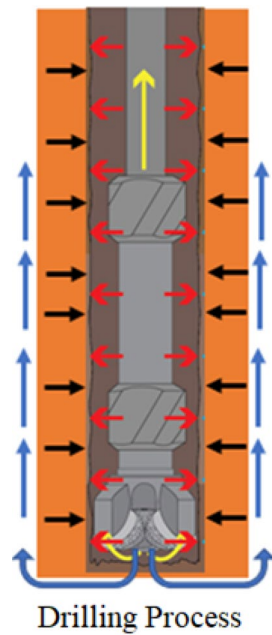
Figure 1. Schematic representation of the drilling process.
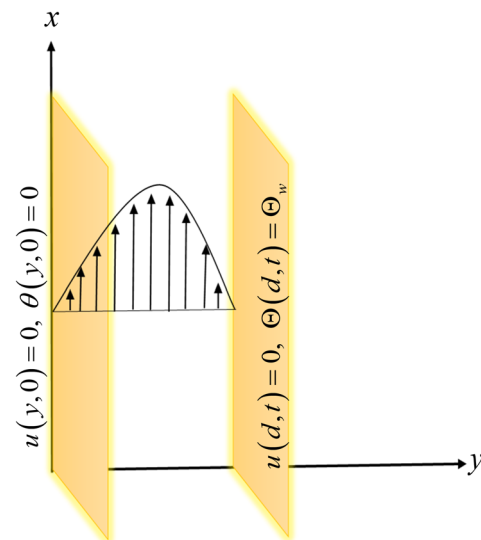

Figure 2. Schematic diagram of the flow.

several reasons, the solutions obtained here are significant. These solutions can be used to verify the precision of their results by experimentalists in various water filtration process applications. Engineers can utilize these findings to decrease the number of experiments and time spent on practical work by altering different factors during the drilling process. Al_2O_3 was chosen for its capacity to improve drilling mud rheological, electrical, and thermal characteristics. Because of their shape, graphite (Gr) is used to offer reduced filtrate loss. Furthermore, the Al_2O_3, Gr combination is non-hazardous and ecologically safe, making it ideal for usage in sensitive settings and applications, the drilling process is represented in Fig. 1.

Model formulation

Let us suppose an incompressible Newtonian viscous hybrid nanofluid between two infinite parallel plates. Water is taken as a based fluid with the combination of graphite and aluminium oxide nanoparticles. The distance between plates is d in a coordinate system. It is assumed that both plates are at rest and the temperature of the left plate is Θ_0, while the right plate temperature is Θ_w. The flow of the fluid is due to free convection as shown in Fig. 2.

The Reynolds number is neglected, and no pressure gradient is assumed in the direction of flow. Maxwell's relations for the magnetic field and Newton's second law for velocity. Maxwell's set of equations is as follow[33]:

$$\left.\begin{array}{l} \nabla \cdot \overrightarrow{B} = 0, \\ \nabla \cdot \overrightarrow{E} = -\frac{\partial \overrightarrow{B}}{\partial t}, \\ \nabla \cdot \overrightarrow{B} = \mu_0 \overrightarrow{J}, \end{array}\right\} \tag{1}$$

where

$$\overrightarrow{J} = \sigma_0\left[\overrightarrow{E} + \overrightarrow{V} \times \overrightarrow{B}\right], \tag{2}$$

Moreover, the electromagnetic force is described as[33]

$$\overrightarrow{F_{em}} = \overrightarrow{J} \times \overrightarrow{B} = \sigma_0\left[\overrightarrow{E} + \overrightarrow{V} \times \overrightarrow{B}\right] \times \overrightarrow{B} = -\sigma B_0^2 u(y,t)\mathrm{i}, \tag{3}$$

where i is the unit vector in the x-direction. And $\overrightarrow{V} = (u(y,t)\mathrm{i}, 0, 0)$ By incorporating $\overrightarrow{F_{em}}$ in momentum equation of unsteady incompressible we get the following set of partial differential equation[34]:

$$\rho_{hnf}\frac{\partial u(y,t)}{\partial t} = \mu_{hnf}\frac{\partial^2 u(y,t)}{\partial y^2} + g(\rho\beta_\Theta)_{hnf}(\Theta u(y,t) - \Theta_0) - \sigma_{hnf}B_0^2 u(y,t) \\ - \frac{\mu_{hnf}}{k}u(y,t). \tag{4}$$

where

$$\mu_{hnf} = \frac{\mu_f}{(1 - \phi_{s1})^{2.5}(1 - \phi_{s2})^{2.5}},$$

$$\rho_{hnf} = \phi_2\rho_{s2} + (1 - \phi_{s2})\big\{(1 - \phi_{s1})\rho_f + \phi_{s1}\rho_{s1}\big\},$$

$$(\rho\beta_\Theta)_{hnf} = \phi_{s2}(\rho\beta_\Theta)_{s2} + (1 - \phi_{s2})\big\{(1 - \phi_{s1})(\rho\beta_\Theta)_f + \phi_{s1}(\rho\beta_\Theta)_{s1}\big\}.$$

The energy equation is

$$\left(\rho C_p\right)_{hnf}\frac{\partial \Theta(y,t)}{\partial t} = K_{hnf}\frac{\partial^2 \Theta(y,t)}{\partial y^2} + Q_0(\Theta - \Theta_0), \tag{5}$$

where $\sigma_{hnf}, \left(\rho C_p\right)_{hnf}$ and K_{hnf} are the heat capacity and thermal conductivity of nanofluids defined as[35]:

$$\sigma_{hnf} = \sigma_{bf}\left\{\frac{\sigma_{s2}(1 + 2\phi_{s2}) + 2\sigma_{bf}(1 - \phi_{s2})}{\sigma_{s2}(1 - \phi_{s2}) + \sigma_{bf}(2 + \phi_{s2})}\right\},$$

$$\sigma_{bf} = \sigma_f\left\{\frac{\sigma_{s1}(1 + 2\phi_{s1}) + 2\sigma_f(1 - \phi_{s1})}{\sigma_{s1}(1 - \phi_{s1}) + \sigma_f(2 + \phi_{s1})}\right\}$$

$$\left(\rho C_p\right)_{hnf} = \phi_{s2}\left(\rho C_p\right)_{s2} + (1 - \phi_{s2})\big\{(1 - \phi_{s1})\left(\rho C_p\right)_f + \phi_{s1}\left(\rho C_p\right)_{s1}\big\},$$

$$\frac{K_{bf}}{K_f} = \left\{\frac{K_{s1} + (m - 1)K_f - (m - 1)\phi_{s1}\left(K_f - K_{s1}\right)}{K_{s1} + (m - 1)K_f + \phi_{s1}\left(K_f - K_{s1}\right)}\right\},$$

$$\frac{K_{hnf}}{K_{bf}} = \left\{\frac{K_{s2} + (m - 1)K_{bf} - (m - 1)\phi_{s2}\left(K_{bf} - K_{s2}\right)}{K_{s2} + (m - 1)K_{bf} + \phi_{s2}\left(K_{bf} - K_{s2}\right)}\right\}.$$

The physical IBC are:

$$u(y,0) = 0, \quad \Theta(y,0) = \Theta_0 \text{ for all } y \geq 0, \tag{6}$$

$$u(0,t) = 0, \quad \Theta(0,t) = \Theta_0, \quad t > 0, \tag{7}$$

$$u(d,t) = 0, \quad \Theta(d,t) = \Theta_w, \quad t > 0, \tag{8}$$

the subsequent dimensionless variables are introduced for non-dimensionalization:

$$t^* = \frac{v_f}{d^2}t, \quad \theta = \frac{\Theta - \Theta_0}{\Theta_w - \Theta_0}, y^* = \frac{y}{d}, \quad u^* = \frac{d}{v_f}u, \tag{9}$$

used into Eqs. (2)–(8), we get (for simplicity dropped * sign)

$$g_1 \frac{\partial u}{\partial t}(y,t) = g_2 \frac{\partial^2 u}{\partial y^2}(y,t) + g_3 Gr_1 \theta(y,t) - g_6 Mu(y,t) - \frac{1}{k_1} g_2 u(y,t), \tag{10}$$

$$g_4 \Pr \frac{\partial \theta(y,t)}{\partial t} = Q\theta(y,t) + g_5 \frac{\partial^2 \theta(y,t)}{\partial y^2}. \tag{11}$$

$$u(y,0) = 0, \ \ \theta(y,0) = 0 \text{ for all } y \geq 0, \tag{12}$$

$$u(0,t) = 0, \ \ \theta(0,t) = 0, \ t > 0, \tag{13}$$

$$u(1,t) = 0, \ \ \theta(1,t) = 1, \ t > 0, \tag{14}$$

where

$$\Pr = \frac{\mu_f (C_p)_f}{K_f}, g_1 = (1 - \phi_{s2})\left(1 - \phi_{s1} + \phi_{s1}\frac{\rho_{s1}}{\rho_f}\right) + \phi_{s2}\frac{\rho_{s2}}{\rho_f}, Gr_1 = \frac{g(\beta_\Theta)_f (\Theta_w - \Theta)_\infty}{U^3},$$

$$g_2 = \frac{1}{(1 - \phi_{s1})^{2.5}(1 - \phi_{s2})^{2.5}}, g_3 = (1 - \phi_{s2})\left\{1 - \phi_{s1} + \phi_{s1}\frac{(\rho\beta_\Theta)_{s1}}{(\rho\beta_\Theta)_f}\right\} + \phi_{s2}\frac{(\rho\beta_\Theta)_{s2}}{(\rho\beta_\Theta)_f}, Q = \frac{Q_0 d^2}{K_f}$$

$$g_4 = (1 - \phi_{s2})\left\{1 - \phi_{s1} + \phi_{s1}\frac{(\rho C_p)_{s1}}{(\rho C_p)_f}\right\} + \phi_2\frac{(\rho C_p)_{s2}}{(\rho C_p)_f}, g_5 = \left(\frac{K_{hnf}}{K_f}\right), g_6 = \frac{\sigma_{hnf}}{\sigma_{bf}}, k_1 = \frac{k}{d^2}$$

$$\frac{K_{hnf}}{K_f} = \left\{\frac{K_{s1} + (m-1)K_f - (m-1)\phi_{s1}(K_f - K_{s1})}{K_{s1} + (m-1)K_f + \phi_{s1}(K_f - K_{s1})}\right\}\left\{\frac{K_{s2} + (m-1)K_{bf} - (m-1)\phi_{s2}(K_{bf} - K_{s2})}{K_{s2} + (m-1)K_{bf} + \phi_{s2}(K_{bf} - K_{s2})}\right\}.$$

Solution with fractional model

The flow chart of the problem is summarized in Fig. 3. Furthermore, the Caputo time fractional model of Eqs. (10) and (11) as follows:

$$g_1 {}^C D_t^\alpha u(y,t) = g_2 \frac{\partial^2 u(y,t)}{\partial y^2} + g_3 Gr_1 \theta(y,t) - g_6 Mu(y,t) - \frac{1}{k_1} g_2 u(y,t), \tag{15}$$

$$g_4 \Pr {}^C D_t^\alpha \theta(y,t) = g_5 \frac{\partial^2 \theta(y,t)}{\partial y^2} + Q\theta(y,t). \tag{16}$$

where

$$^C D_t^\alpha f(y,t) = \begin{cases} \frac{1}{\Gamma(1-\alpha)} \int_0^t \frac{1}{(t-\tau)^\alpha} \frac{\partial f(y,\tau)}{\partial \tau} d\tau, \ 0 < \alpha < 1 \\ \frac{\partial f(y,\tau)}{\partial \tau}, \qquad\qquad\qquad \alpha = 1. \end{cases}$$

Apply the Laplace transform of Eqs. (15) and (16) and simplify we get:

$$\overline{\theta}(y,q) = \frac{\sinh\left(y\sqrt{\frac{g_9 q}{q+g_8} + \frac{Q}{g_5}}\right)}{\sinh\left(\sqrt{\frac{g_9 q}{q+g_8} + \frac{Q}{g_5}}\right)} \frac{1}{q} \tag{17}$$

$$\overline{u}(y,q) = \frac{1}{q} \frac{\frac{g_3}{g_2} Gr_1}{\frac{g_9 q}{q+g_8} + \frac{Q}{g_5} - \sqrt{\frac{\frac{g_3}{g_2} g_1 q}{q+g_8} + \frac{g_{10}}{g_2}}} \left[\frac{\sinh\left(y\sqrt{\frac{\frac{g_3}{g_2} g_1 q}{q+g_8} + \frac{g_{10}}{g_2}}\right)}{\sinh\left(\sqrt{\frac{\frac{g_3}{g_2} g_1 q}{q+g_8} + \frac{g_{10}}{g_2}}\right)} - \frac{\sinh\left(y\sqrt{\frac{g_9 q}{q+g_8} + \frac{Q}{g_5}}\right)}{\sinh\left(\sqrt{\frac{g_9 q}{q+g_8} + \frac{Q}{g_5}}\right)} \right], \tag{18}$$

Equations (17) and (18) present the solutions of Eqs. (15) and (16) in the transformed variable q. To obtain the inverse Laplace transform by using the inversion method by[36–39], we get
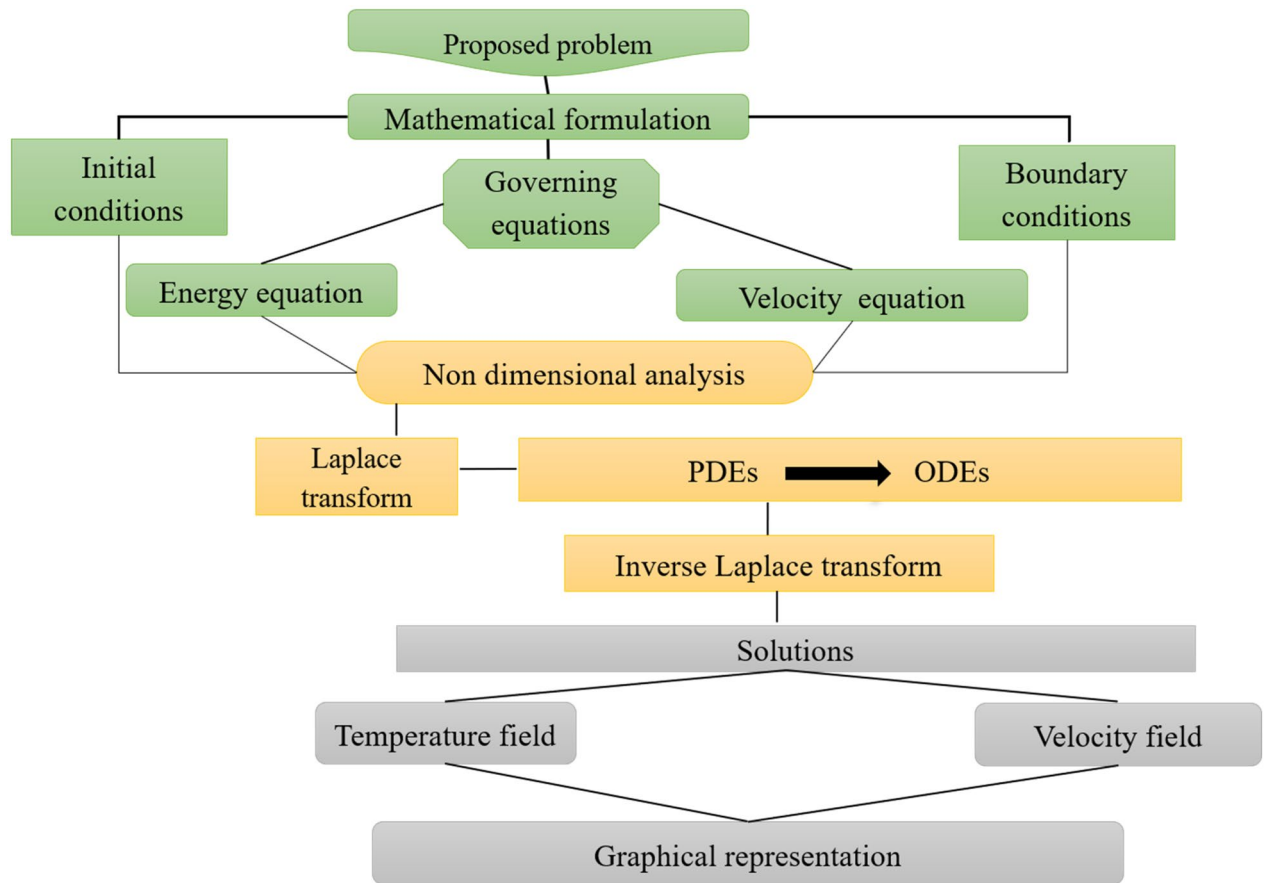
Figure 3. Flow chart of the steps-wise procedure.

$$\theta(y,t) = \frac{2}{t} \sum_{j=1}^{N} \text{Re}\left\{ K_j \overline{\theta}\left(y, \frac{\alpha_j}{t}\right) \right\} \qquad (19)$$

$$u(y,t) = \frac{2}{t} \sum_{j=1}^{N} \text{Re}\left\{ K_j \overline{u}\left(y, \frac{\alpha_j}{t}\right) \right\} \qquad (20)$$

where K_j and α_j are given as;

j	K_j	α_j
1	$12.83767675 + i\,1.666063445$	$-36{,}902.0821 + i\,196{,}990.4257$
2	$12.22613209 + i\,5.012718792$	$61{,}277.02524 - i\,95{,}408.62551$
3	$10.93430308 + i\,8.409673116$	$-28{,}916.56288 + i\,18{,}169.18531$
4	$8.776434715 + i\,11.92185389$	$4655.361138 - i\,1.901528642$
5	$5.225453361 + i\,15.72952905$	$-118.7414011 - i\,141.3036911$

Graphical results and discussion
See Figs. 3, 4, 5, 6, 7, 8, 9, 10, 11 and 12.

Results and discussion
The problem of hybrid nanofluid is solved by using the Laplace transform method. Results are computed and discussed for several embedded parameters. Results are based on the nanoparticle's thermophysical properties in Table 1. Results plotted in Fig. 4 reflects the effect of fractional parameter α on velocity and temperature distributions. Different graphs for different values of α obtained for velocity and temperature profiles. These graphs are obtained for various values of α while keeping other parameters constants. In addition, each graph is made for a distinct value of α, which represents a solution so in this manner we have obtained various solutions. For the
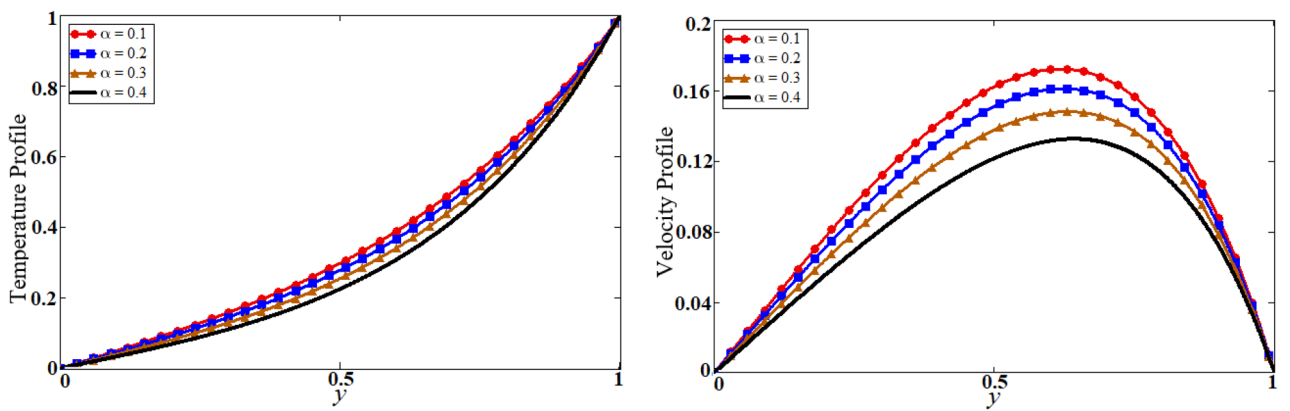
Figure 4. Results of the fractional parameter α on temperature and velocity profile.
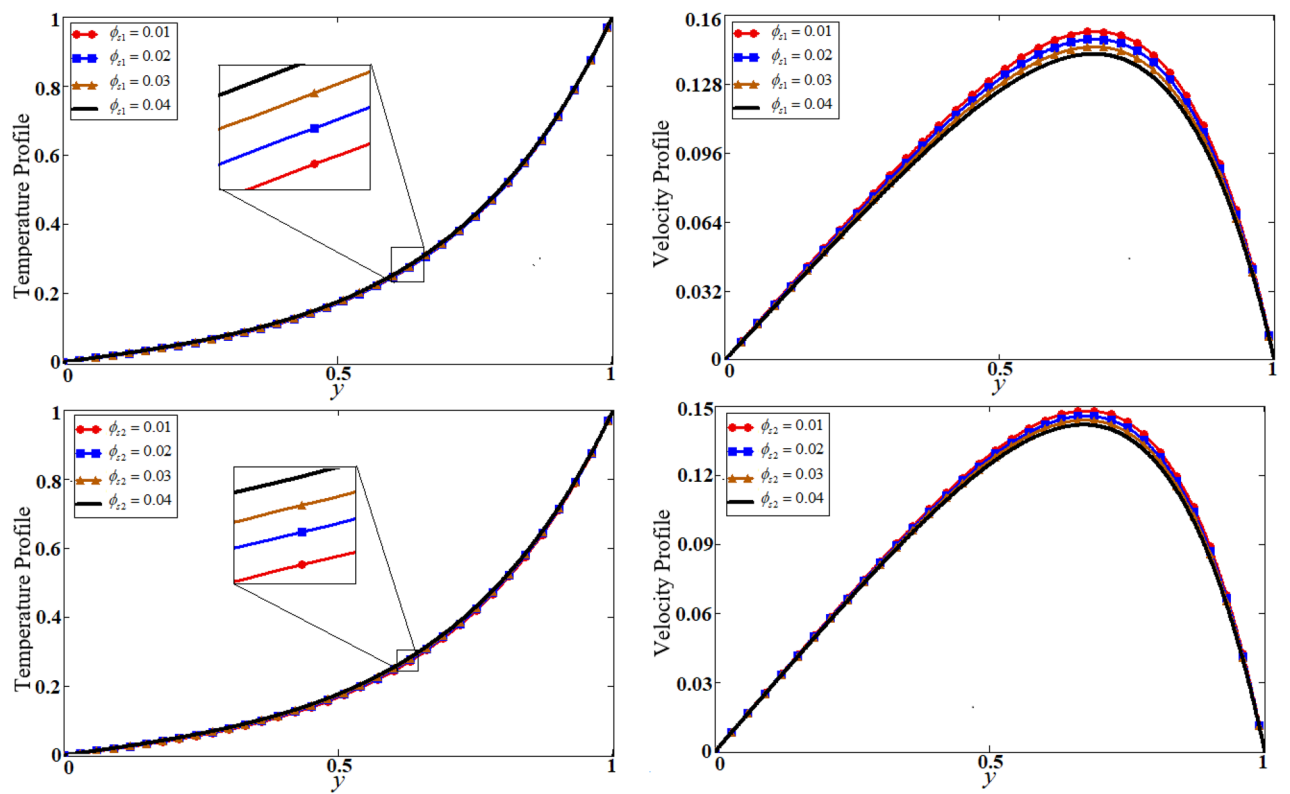

Figure 5. Results of volume fractional of both nanoparticles on temperature and velocity.
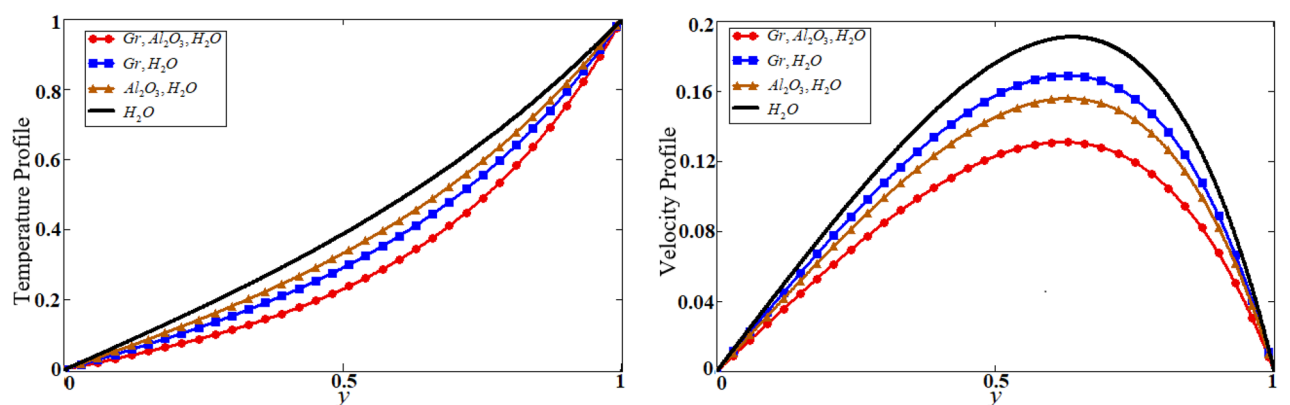

Figure 6. Comparison of hybrid nanofluid with nanofluid on temperature and velocity profile.
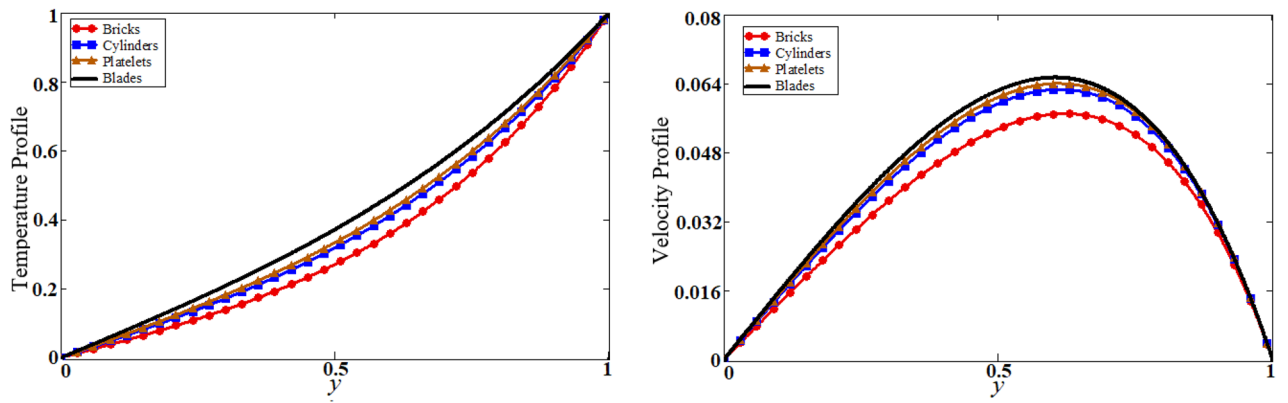
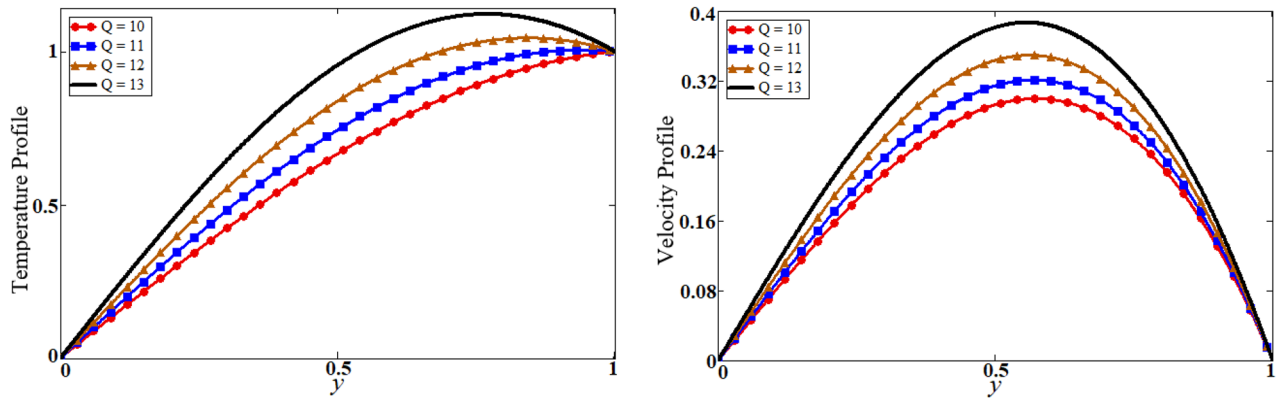**Figure 7.** The shape effect of nanoparticles on temperature and velocity.

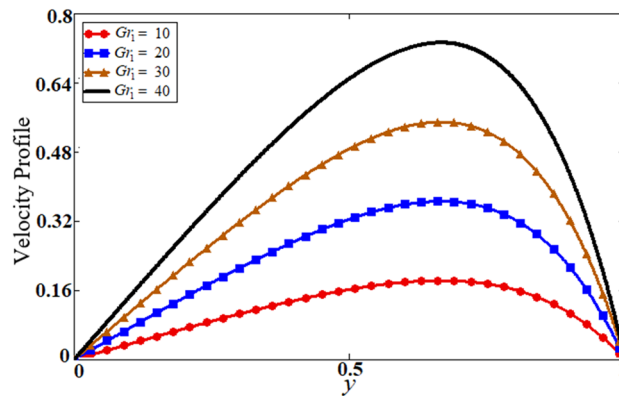**Figure 8.** Results of heat generation Q on temperature and velocity.

Figure 9. Results of Gr_1 on velocity.

experimentalists, it is easy to select the best curve fitting graph, which can be in good agreement with the results of real data. When ϕ is increased from 0.01 to 0.04, the velocity of the hybrid nanofluid is decreased for both particles, ϕ_{s1} for one particle and ϕ_{s2} for the second one. Physically this phenomenon says that with increasing values of volume fraction, the viscous forces become stronger due to which velocity retards. This physical trend is noted in Fig. 5 for both nanoparticles volume fractions. Which makes a strong agreement with the physics of the volume fraction of hybrid nanofluids. The comparison of Al_2O_3, Gr (hybrid nanofluid) is shown with respect to water-base Gr and Al_2O_3 nanofluid in Fig. 6. It is observed that the velocity of the Al_2O_3, Gr (hybrid nanofluid) is lower as compared to other nanofluids. Physically, this is true because the density of Al_2O_3, Gr (hybrid nanofluid) is greater than the density of other nanofluids which is a factor to decrease the velocity. Moreover, the temperature distribution shows the same behavior as that of the velocity profile. As Al_2O_3, Gr (hybrid nanofluid) has higher thermal conductivity than other nanofluids but less density. Consequently, Al_2O_3, Gr (hybrid nanofluid)
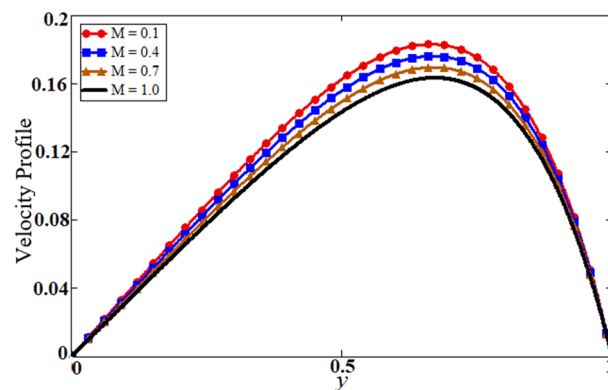
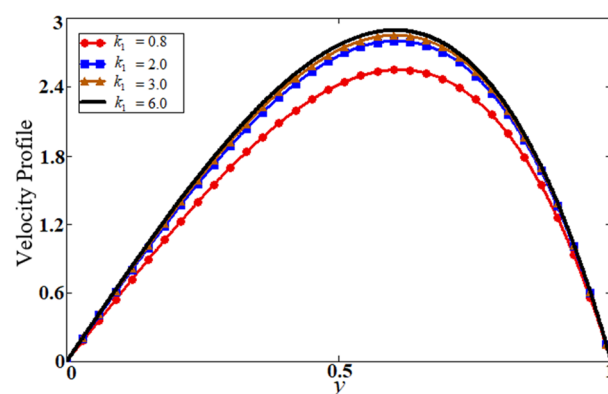**Figure 10.** Results of magnetic parameter M on velocity.

Figure 11. Results of porosity parameter k_1 on velocity.
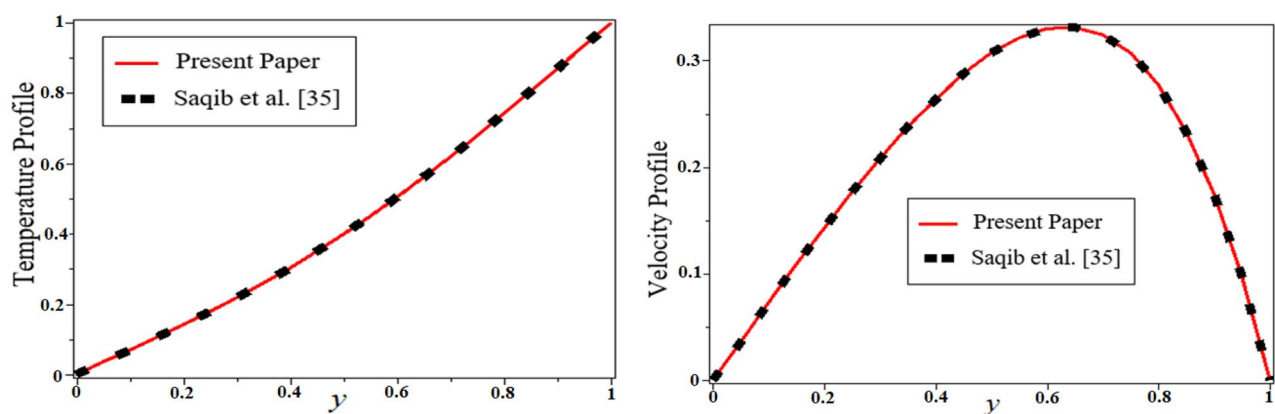

Figure 12. Comparison plot of the present solution with Saqib et al.[40].

transfers more heat compared to other nanofluids and are less dense, as a result, the temperature distributions of Al_2O_3, Gr (hybrid nanofluid) is lower than other nanofluids. The effect of the shape factor on the velocity and temperature profiles has been depicted in Fig. 7. The hydrogen bonding of hybrid nanofluid produces an important argument in thermal conductivity thus the velocity and temperature distribution are enhanced. The temperature profile for blade shape hybrid nanoparticles is maximum while for brick shape nanoparticles the temperature distribution is minimum. Similarly, the velocity profile for blade shape is maximum and minimum for brick shape nanoparticles. Figure 8 illustrates the influence of heat generation in temperature and velocity field, it is notified that heat generation boosts the temperature and velocity. When Q is set to a higher value, it

Material	Base fluids	Nanoparticles	
	Water	Al$_2$O$_3$	Gr
$\rho\left(\text{kg/m}^3\right)$	997.1	3970	1300
$c_p\left(\text{J/kg K}\right)$	4179	765	830
$K\left(\text{W/m K}\right)$	0.613	40	12
$\beta \times 10^{-5}\left(\text{K}^{-1}\right)$	21	0.85	2.83
$\sigma\left(\Omega\text{m}\right)$	0.05	3.5*10^6	3.3
Pr	6.2	–	–

Table 1. Base fluid and nanoparticles thermophysical properties[9].

$\phi_{s1} + \phi_{s2}$	Nu	%age
0	0.27	
0.01	0.294	8.888889
0.02	0.319	18.14815
0.03	0.344	27.40741
0.04	0.371	37.40741
Different fluids	**Nu**	**%age**
Water	0.27	0
Gr	0.313	15.92593
Al$_2$O$_3$	0.321	18.88889
Gr-Al$_2$O$_3$	0.371	37.40741
Shape, m	**Nu**	**%age**
Bricks, 3.9	0.287	0
Cylinders, 4.9	0.296	3.135889
Platelets, 5.7	0.303	5.574913
Blades, 8.6	0.319	11.14983

Table 2. The percentage variation of Nusselt number.

indicates that the device has absorbed more heat, resulting in a weaker intermolecular attractive force, which causes the temperature and velocity profiles to rise. Figure 9 reflects the influence of Gr_1 on the velocity of hybrid nanofluid. Gr_1 is the ratio of thermal to viscous forces, the dominancy of thermal forces for the fluid velocity for enhancement? That is why the increasing behavior of velocity of hybrid nanofluid is pictured in Fig. 9. Figure 10 stipulates that enhancing the magnetic parameter M provides a considerable hindrance to the flow behavior. This hindrance is due to the fact that enlargement of M strengthens the Lorentz forces, which by nature are resistive forces. Therefore, due to these strong resistive forces' retardation occurs in the fluid flow, and a decrease in boundary layer thickness is seen.

The last Fig. 11 illustrates the effect of the porosity parameter k_1 on velocity profile, which enhances the velocity of the fluid. This is due to a decrease in the resistance of the porous medium, which leads to an increase in the thickness of the momentum boundary layer. By putting $\alpha = 0.5$, $M = 1.5$, $Gr = 5$, $k_1 = 15$, $t = 1$, $Q = 0$ and $\phi_{s1} = \phi_{s2} = 0$ our solution is reduced to the solution of Saqib et al.[40], which is presented in Fig. 12. Table 2 highlights the variation of Nusselt number for classical, unitary, and hybrid nanofluids nanoparticles, comparative analysis with nanofluid and shape effect of nanoparticles. It is observed that the enhancement of the rate of heat transfer is boosting up to 37.40741% by using hybrid nanofluid compared to unitary nanofluids, and up to 11.14983% by adding differently shaped nanoparticles in the base fluids. The variation of skin fraction for both plates is present in Table 3. It is observed from this table that increasing the volume fraction of nanofluid increases the skin faction on a left plate while the opposite behavior on the right plate. It is also clear that blades shaped nanoparticles have a high skin fraction on a left plate while Brick's shape nanoparticles have a high skin fraction on the right plate.

Summery

In the water filtration process application, this mathematical model is developed and analyzed with the combination of nanoparticles which make hybrid nanofluid. The results (graphical and tabulated) are purely obtained by numerical inversion of the Laplace transform. The different parameters are analyzed for the velocity and temperature profile. The comparison is also explored for nanofluid and hybrid nanofluid with graphite and aluminium oxide nanoparticles. The main outcomes are as follows.

$\phi_{s1} + \phi_{s2}$	Cf at y = 0	Cf at y = 1
0	0.635	− 1.692
0.01	0.667	− 1.743
0.02	0.719	− 1.841
0.03	0.795	− 2
0.04	0.887	− 2.196
Different fluids	**Cf at y = 0**	**Cf at y = 1**
Water	0.635	− 1.692
Gr	0.66	− 1.737
Al_2O_3	0.638	− 1.689
Gr-Al_2O_3	0.667	− 1.743
Shape, m	**Cf at y = 0**	**Cf at y = 1**
Bricks, 3.9	0.667	− 1.743
Cylinders, 4.9	0.674	− 1.753
Platelets, 5.7	0.679	− 1.76
Blades, 8.6	0.7	− 1.796

Table 3. The variation of skin fraction on both plates.

- The fractional parameter provides the range of solution for temperature and velocity profile which makes the analysis more general as compared to the classical one.
- The hybrid nanofluid has enhanced the temperature and retard the velocity, which helps in the rate of heat transfer during the drilling process.
- The shape effect of nanoparticles reduced the temperature and velocity profile, which means that different shapes of nanoparticles should be used to control the temperature and velocity of the hybrid nanofluid during the filtration process by adding different shapes of the nanoparticle.
- Dissolving the hybrid nanocomposite (Al_2O_3, Gr) in a water-base enhances the rate of heat transfer up to 37.40741%, which is higher than unitary nanofluid.
- The blade's shape of nanoparticles enhances the rate of heat transfer up to 11.14983% rather than other shapes of nanoparticles during the filtration process.
- The skin fraction on both plates can be controlled by adding hybrid nanofluid, the volume fraction of nanoparticles, and by adding different shapes of nanoparticles.

Lastly, I endorse some suggestions for future research to the readers as below.

- The following concept can be applied to various geometries of calendrical coordinates.
- One way to explore the same concept for different types of fluids with slip boundary conditions.
- Furthermore, some new fractional derivatives can be used to more effectively summarise present fluid models along with concertation equations.

Data availability
Data of this study will be made available from the corresponding author on reasonable request.

References
1. Belhocine, A. & Omar, W. W. Numerical study of heat convective mass transfer in a fully developed laminar flow with constant wall temperature. *Case Stud. Therm. Eng.* **6**, 116–127 (2015).
2. Belhocine, A. & Omar, W. Z. W. Analytical solution and numerical simulation of the generalized Levèque equation to predict the thermal boundary layer. *Math. Comput. Simul.* **180**, 43–60 (2021).
3. Belhocine, A. Numerical study of heat transfer in fully developed laminar flow inside a circular tube. *Int. J. Adv. Manuf. Technol.* **85**(9), 2681–2692 (2016).
4. Belhocine, A. & Wan Omar, W. Z. An analytical method for solving exact solutions of the convective heat transfer in fully developed laminar flow through a circular tube. *Heat Transf. Asian Res.* **46**(8), 1342–1353 (2017).
5. Belhocine, A. & Abdullah, O. I. Numerical simulation of thermally developing turbulent flow through a cylindrical tube. *Int. J. Adv. Manuf. Technol.* **102**(5), 2001–2012 (2019).
6. Saqib, M., Ali, F., Khan, I., Sheikh, N. A. & Khan, A. Entropy generation in different types of fractionalized nanofluids. *Arab. J. Sci. Eng.* **44**(1), 531–540 (2019).
7. Choi, S. U. & Eastman, J. A. *Enhancing thermal conductivity of fluids with nanoparticles* (No. ANL/MSD/CP-84938; CONF-951135–29). Argonne National Lab., IL (United States) (1995).
8. Gbadamosi, A. O. *et al.* Recent advances and prospects in polymeric nanofluids application for enhanced oil recovery. *J. Ind. Eng. Chem.* **66**, 1–19 (2018).

9. Elbashbeshy, E. M. A., Emam, T. G. & Abdel-Wahed, M. S. Effect of heat treatment process with a new cooling medium (nanofluid) on the mechanical properties of an unsteady continuous moving cylinder. *J. Mech. Sci. Technol.* **27**(12), 3843–3850 (2013).
10. Khajehzadeh, M., Moradpour, J. & Razfar, M. R. Influence of nanofluids application on contact length during hard turning. *Mater. Manuf. Processes* **34**(1), 30–38 (2019).
11. Sharif, S., Sadiq, I. O., Yusof, N. M. & Mohruni, A. S. A review of minimum quantity lubrication technique with nanofluids application in metal cutting operations. *Int. J. Adv. Sci. Eng. Inf. Technol.* **7**(2), 587–593 (2017).
12. Pandya, N. S., Shah, H., Molana, M. & Tiwari, A. K. Heat transfer enhancement with nanofluids in plate heat exchangers: A comprehensive review. *Eur. J. Mech.-B/Fluids* **81**, 173–190 (2020).
13. Sheremet, M. A., Pop, I. & Mahian, O. J. I. J. O. H. Natural convection in an inclined cavity with time-periodic temperature boundary conditions using nanofluids: Application in solar collectors. *Int. J. Heat Mass Transf.* **116**, 751–761 (2018).
14. Ali, F., Khan, I., Sheikh, N. A. & Gohar, M. Exact solutions for the Atangana-Baleanu time-fractional model of a Brinkman-type nanofluid in a rotating frame: Applications in solar collectors. *Eur. Phys. J. Plus* **134**(3), 1–18 (2019).
15. Krishna, M. V. & Chamkha, A. J. Hall and ion slip effects on Unsteady MHD Convective Rotating flow of Nanofluids—Application in Biomedical Engineering. *J. Egyptian Math. Soc.* **28**(1), 1–15 (2020).
16. Molana, M. A comprehensive review on the nanofluids application in the tubular heat exchangers. *Am. J. Heat Mass Transf.* **3**(5), 352–381 (2016).
17. Molana, M. On the nanofluids application in the automotive radiator to reach the enhanced thermal performance: A review. *Am. J. Heat Mass Transf.* **4**(4), 168–187 (2017).
18. Sajid, M. U. & Ali, H. M. Recent advances in application of nanofluids in heat transfer devices: A critical review. *Renew. Sustain. Energy Rev.* **103**, 556–592 (2019).
19. Sundar, L. S., Sharma, K. V., Singh, M. K. & Sousa, A. C. M. Hybrid nanofluids preparation, thermal properties, heat transfer and friction factor–a review. *Renew. Sustain. Energy Rev.* **68**, 185–198 (2017).
20. Sidik, N. A. C., Xian, H. W., Aid, S. R., Ken, T. L. & Asako, Y. Review on preparation techniques, properties and performance of hybrid nanofluid in recent engineering applications. *J. Adv. Res. Fluid Mech. Therm. Sci.* **45**(1), 1–13 (2018).
21. Ghadikolaei, S. S., Yassari, M., Sadeghi, H., Hosseinzadeh, K. & Ganji, D. D. Investigation on thermophysical properties of Tio2–Cu/H2O hybrid nanofluid transport dependent on shape factor in MHD stagnation point flow. *Powder Technol.* **322**, 428–438 (2017).
22. Yıldız, Ç., Arıcı, M. & Karabay, H. Comparison of a theoretical and experimental thermal conductivity model on the heat transfer performance of Al2O3-SiO2/water hybrid-nanofluid. *Int. J. Heat Mass Transf.* **140**, 598–605 (2019).
23. Hayat, T. & Nadeem, S. Heat transfer enhancement with Ag–CuO/water hybrid nanofluid. *Results Phys.* **7**, 2317–2324 (2017).
24. Muhammad, K., Hayat, T., Alsaedi, A. & Ahmad, B. Melting heat transfer in squeezing flow of basefluid (water), nanofluid (CNTs+ water) and hybrid nanofluid (CNTs+ CuO+ water). *J. Therm. Anal. Calorim.* **143**, 1–18 (2020).
25. Khan, U., Shafiq, A., Zaib, A. & Baleanu, D. Hybrid nanofluid on mixed convective radiative flow from an irregular variably thick moving surface with convex and concave effects. *Case Stud. Therm. Eng.* **21**, 100660 (2020).
26. Hamid, M., Zubair, T., Usman, M. & Haq, R. U. Numerical investigation of fractional-order unsteady natural convective radiating flow of nanofluid in a vertical channel. *AIMS Math.* **4**(5), 1416–1429 (2019).
27. Hussanan, A., Salleh, M. Z., Khan, I. & Chen, Z. M. Unsteady water functionalized oxide and non-oxide nanofluids flow over an infinite accelerated plate. *Chin. J. Phys.* **62**, 115–131 (2019).
28. Biswas, N., Sarkar, U. K., Chamkha, A. J. & Manna, N. K. Magneto-hydrodynamic thermal convection of Cu–Al 2 O 3/water hybrid nanofluid saturated with porous media subjected to half-sinusoidal nonuniform heating. *J. Therm. Anal. Calorim.* **143**(2), 1727–1753 (2021).
29. Rostami, S., Toghraie, D., Shabani, B., Sina, N. & Barnoon, P. Measurement of the thermal conductivity of MWCNT-CuO/water hybrid nanofluid using artificial neural networks (ANNs). *J. Therm. Anal. Calorim.* **143**(2), 1097–1105 (2021).
30. Suganya, S., Muthtamilselvan, M. & Alhussain, Z. A. Activation energy and Coriolis force on Cu–TiO2 /water hybrid nanofluid flow in an existence of nonlinear radiation. *Appl. Nanosci.* **11**(3), 933–949 (2021).
31. Mousavi, S. M., Rostami, M. N., Yousefi, M. & Dinarvand, S. Dual solutions for MHD flow of a water-based TiO2-Cu hybrid nanofluid over a continuously moving thin needle in presence of thermal radiation. *Rep. Mech. Eng.* **2**(1), 31–40 (2021).
32. Rashid, U. *et al.* Study of (Ag and TiO2)/water nanoparticles shape effect on heat transfer and hybrid nanofluid flow toward stretching shrinking horizontal cylinder. *Results Phys.* **21**, 103812 (2021).
33. Saqib, M., Khan, I. & Shafie, S. Generalized magnetic blood flow in a cylindrical tube with magnetite dusty particles. *J. Magn. Magn. Mater.* **484**, 490–496 (2019).
34. Khan, I., Hussanan, A., Saqib, M. & Shafie, S. Convective heat transfer in drilling nanofluid with Clay nanoparticles: Applications in water cleaning process. *BioNanoScience* **9**(2), 453–460 (2019).
35. Khan, A. M. *et al.* Energy-based cost integrated modelling and sustainability assessment of Al-GnP hybrid nanofluid assisted turning of AISI52100 steel. *J. Clean. Prod.* **257**, 120502 (2020).
36. Zakian, V. Numerical inversion of Laplace transform. *Electron. Lett.* **5**, 120–121 (1969).
37. Sheikh, N. A., Chuan Ching, D. L., Khan, I., Ahmad, A. & Ammad, S. Concrete based jeffrey nanofluid containing zinc oxide nanostructures: Application in cement industry. *Symmetry* **12**(6), 1037 (2020).
38. Wang, Q. & Zhan, H. On different numerical inverse Laplace methods for solute transport problems. *Adv. Water Resour.* **75**, 80–92 (2015).
39. Sun, H., Chen, W., Li, C. & Chen, Y. Finite difference schemes for variable-order time fractional diffusion equation. *Int. J. Bifurc. Chaos* **22**(04), 1250085 (2012).
40. Saqib, M., Khan, I. & Shafie, S. Application of Atangana-Baleanu fractional derivative to MHD channel flow of CMC-based-CNT's nanofluid through a porous medium. *Chaos, Solitons Fractals* **116**, 79–85 (2018).
41. Tenreiro Machado, J. A., Silva, M. F., Barbosa, R. S., Jesus, I. S., Reis, C. M., Marcos, M. G. & Galhano, A. F. Some applications of fractional calculus in engineering. *Math. Probl. Eng.* (2010).

Acknowledgements

Author contributions

D.K. and I.K. formulated the problem. D.K., A.K. solved the problem. D.K. performed the investigations. W.W. and P.K. supervision, P.K. funding, P.K. and M.A. wrote the paper.

Competing interests

The authors declare no competing interests.

Additional information

Correspondence and requests for materials should be addressed to P.K.

Reprints and permissions information is available at www.nature.com/reprints.

Publisher's note Springer Nature remains neutral with regard to jurisdictional claims in published maps and institutional affiliations.